A Monte-Carlo Study of Ring Formation and Molecular Configurations during Step Growth on a Lattice in Three Dimensions

Allan H. Fawcett,* Richard A. W. Mee, and Frederick V. McBride

School of Chemistry, Institute of Computer-Based Learning, The Queen's University of Belfast, BT9 5AG, Northern Ireland, U.K.

Received July 11, 1994; Revised Manuscript Received October 31, 1994[⊗]

ABSTRACT: The formation of ring and chain molecules during an irreversible step growth polymerization has been modeled on a three-dimensional 26-choice cubic lattice, and examined by the Monte-Carlo method. The limiting value of the extent of reaction was found to be $p = 0.98333$ (±0.00002) in this static simulation, when all neighboring pairs of monomers and end groups had reacted mutually to form bonds. Then the mean number of lattice sites within a molecule was 60, which may correspond to a molecular weight of 30 000 for a real polymer. In the simulation the number fraction of molecules found as rings was 0.291 (±0.007), but the weight fraction was much smaller—0.0395 (±0.0016). Ring number distribution functions were found to be closely fitted by a power law, the exponents decreasing as the reaction proceeded, and larger rings then were able to accumulate at a greater rate. The limiting value of the ring distribution exponent was −2.68 (±0.02), a number slightly greater than the appropriate equilibrium distribution value. The chain number distribution functions were perturbed from the conventional Flory expression, particularly toward the end of the process, mainly because the small chains were depleted by the ring formation process. The weight distribution function for all products displays a broad feature for chains and a sharp feature for rings at lower molecular weights. Polydispersities of the distribution functions for rings, for chains, and for both species together were all found to be greater than 2.00. The configurational characteristics of the chains and rings produced by this novel process have been examined and found to lie between self-avoiding walk and the random flight models. They tend toward patterns close to Flory Θ conditions as the reaction proceeds.

Introduction

The formation of ring molecules during a step growth polymerization of difunctional monomers is generally neglected by polymer chemists. Carothers recognized that cyclic monomers might form, for they in particular were identified among the reaction products of, for example, polyester and nylon condensation polymerizations,[1] and while the formation of larger rings was recognized as a possibility, as the compilers of Carothers works have recorded,[1] it was thought to be unlikely on account of the remoteness of the two end groups of chains adopting random configurations. Later, and on a similar basis, Flory also considered that, in competition with chain growth,[2] cyclization might be discounted as a kinetic possibility. The emphasis lay upon the production of long chains, for the very notion of polymerization itself was being established. The equation relating the mean degree of polymerization, $\langle n \rangle$, to the extent of reaction, p,

$$\langle n \rangle = 1/(1 - p) \tag{1}$$

informed Carothers of the idea of creating high molecular weight polymers by condensations reactions of difunctional monomers. In the early treatments of step growth[2,3] the number distribution of chain sizes produced by a kinetic process, neglecting cyclization and assuming equal reactivity of functional groups, was shown to follow the same expression as that given by a thermodynamic equilibrium:

$$N_{c,n} = N_0(1 - p)^2 p^{n-1} \tag{2}$$

where N_0 is the number of residues present initially.

Cyclization at the equilibrium condition has been examined by Jacobson and Stockmayer,[4] who recognized conditions when rings might be present and obtained a simple power law for the distribution of ring number by assuming Gaussian configurational statistics: $N_{r,n} \sim n^{-2.5}$. The deviations from this that are found in the small to medium ring range by experiment on real systems[5] are associated with the fact that real chains occupy discrete conformations, departure from which for the purpose of ring closure causes an extra adverse strain effect over a certain range of molecular weights.

Special conditions apply to the formation of the natural ring macromolecules such as plasmid DNA: they are part of a system of self-replication.[6] Rings do not form at all in the familiar free radical or ionic chain reaction types of the polymerization mechanism, provided that the monomers are mono-unsaturated like styrene: however, as Rempp[7] and Roovers[8] have shown, rings may be obtained by experiment at the end of an anionic polystyrene reaction if the living polymers, having two anionic end groups, are treated with a dihalogen coupling agent under dilute conditions. This is a step growth process leading to cyclic macromonomers. Such ring molecules have different characteristic properties from linear molecules, for example, their glass transition temperature values in the amorphous state are higher than those for linear molecules of the same size when this is small,[9,11] their GPC and melt flow characteristics differ significantly.[12,13] In solution their second virial coefficients are non-zero under what corresponds to Θ conditions for chains[14] and at their Θ temperature the value of the Mark−Houwink exponent, a, is less than 0.50. The possibility of preparing large quantities of small rings by step growth reactions within a stationary phase has been demonstrated: only rings become detached if the monomers are bound.[15] Experiments have now proceeded to prepare quantities of

[⊗] Abstract published in *Advance ACS Abstracts,* January 1, 1995.

0024-9297/95/2228-1481$09.00/0

catenanes.[16] Ring macromolecules are proving to have interesting properties.[17,18]

Competition in step growth between polymerization and ring formation featured in an analytical treatment of step growth kinetics performed by Morawetz,[19] who allowed cyclic monomers to form as in the early view,[1] and a more recent treatment by Mandolini[20] extended the method to rings of up to 12 residues at high dilution, which encourages rings. Ring closure took place at a rate controlled by Gaussian equilibrium chain statistics. We note, however, that both theoretical and experimental studies have suggested that their exists a "hole" in the end-to-end distribution function,[21,22] a feature that might restrict the chances of ring closure. The configurations adopted by a chain in real space are thus important factors in two respects for controlling cyclization.

Our present studies use a model that has kinetic, configurational, and topological features, for we embed the residues in space by placing them upon a lattice, and as the polymerization proceeds we allow rings to form naturally when the conditions are suitable, that is, when the two ends are adjacent to each other and are chosen to be linked by a bond in the random selection process. Since rings form irreversibly from chains by intramolecular reactions, and intermolecular reactions produce chains that may subsequently cyclize, the overall consideration is that if the polymerization process completely consumes the functional groups, the macromolecules will all be in the form of rings. Our lattice model is designed to explore this idea. Once the chains have grown beyond two residues in size, so that they are large enough for ring closure to become a recognizable possibility, at each step growth episode an end group of a particular chain may link with one of another to give a long chain, or it may react with the other end of the same molecule to yield a ring. Despite the small chance of a ring forming at each stage, a chance that falls as the chain size rises[2] and has been described as "vanishingly small",[23] the number fraction of ring molecules increases, for rings accumulate and chains diminish in number during the successive kinetic steps. In a two-dimensional simulation and a preliminary examination in three dimensions about 30% of the molecules that form on the lattices have been found to be rings, by the time the processes ceased.[24,25]

Here we use the Carothers function of eq 1 to measure the course of the polymerization, and we identify rings and chains within the system as it evolves, so that characteristics of the species may be evaluated. We examine the distribution functions for the numbers and weights of the species that are present at different times, using as a standard the Flory equation for the chains and all the species, and for the ring species neglected by the Flory treatment we characterize their distribution functions at various intervals in the reaction. Finally, we study the configurations of the two types of species that are produced by this process, as the molecules are lattice-bound. The kinetics of the reaction, the size of the species, and the configurations of the molecules are intimately related.

Lattice Model

Monomers and the residues of the larger molecules that develop are placed on the vertices of an isotropic cubic lattice of unit spacing. According to a simple algorithm, bonds of three different lengths may form between one randomly chosen unit and one of the set

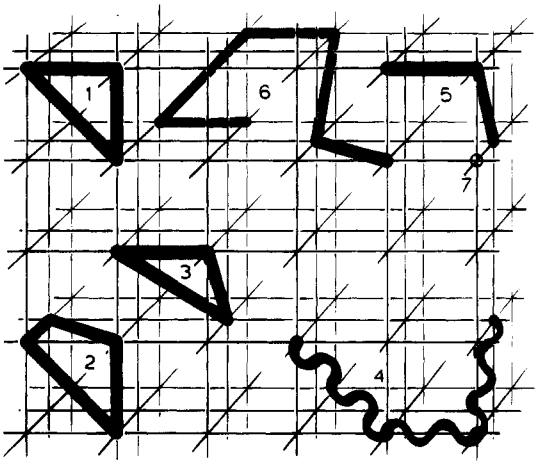

Figure 1. Part of the three-dimensional lattice with typical oligomeric chain and ring molecules displayed upon it. Molecule 4 has a representation of the flexible nature of the bonds between the residues located at the vertices of the lattice.

of its nearest 26 neighbors that again is selected in a random manner. We thus allow bonds to form along the lattice vertices (length 1), along the diagonals of the face of a cube (length $\sqrt{2}$) or along the diagonals joining opposite vertices of a cube (length $\sqrt{3}$). The root mean square value of the bond length $\langle l^2 \rangle^{1/2}$ is $(54/26)^{1/2} \sim 1.441$. Odd numbered as well as even numbered rings are thus permitted, as we show for molecules 1 and 2 on the lattice of Figure 1. A three-membered ring having one of each type of bond length is shown as molecule 3 on the lattice in Figure 1, together with a representation of an oligomer (molecule 4) in which the flexible nature of a segment linking two residues is suggested. A further possibility is that as the number of configurations available to molecules on the simple lattice is maximized, the results may be insensitive to the particular lattice type that has been adopted,[26] and so may represent more reliably the underlying kinetic and topological issues. The adoption of three possible bond lengths is a simple feature of our use of set theory in the Pascal program to list the neighbors of an end group or monomer, resembles one fluctuating bond model,[27] and means that the bonds linking the residues themselves have a certain compressibility and extensibility, as is suggested in molecule 4 of Figure 1. This may be found in real systems where there are several chemical bonds within a residue; furthermore in similar lattice models it has been considered that a lattice bond corresponds to 3−7 chemical residues[27,28] (or to 7−15 chemical bonds).

Besides the simple rule that only one residue may occupy each site, we have the further excluded volume condition that a diagonal bond may not pass through a previously-formed bond, whether that lies in a lattice plane or passes through the center of a cube. In the present treatment all angles between adjacent bonds are allowed, but there are no movements of residues upon the lattice, nor are solvents present. Thus a limit to the extent of reaction achievable arises from the inevitable isolation of unused chemical functionality.

At each unit of time, t, a lattice site is selected at random, and one of the its 26 neighbors is similarly chosen.[29] Depending upon the nature of the structure at each site a bond forms between them with a probability $P = P_1P_2$, where P_1 and P_2 express the probabilities of chemical change at each site. Following the equal reactivity principle,[2] a parameter has the value

of unity if the site is occupied by a monomer, a value of 0.5 if the site is taken by an end group of a chain and has thus reacted once already, and a value of 0 if the residue lies within a molecule, having used up its two valencies. The system corresponds, for example, to the chemical formation of an Si–O–Si link from two Si–O–H groups, as in case 1 of ref 4. (Other chemistries would require different probability parameters.) Toward the end of the simulation, when the rate of reactions had become very small, we set P to unity, and increased the time count by 4 for speed. When only a small fraction of unreacted residues remaind, a procedure identified adjacent pairs of ends and linked them to create a system as fully reacted as possible.

A simple consequence of this approach is that rings form from chains of three or more residues if their ends are on adjacent vertices and they happen to be chosen in a random way. For example, each end of molecule 5 of Figure 1 might react with an end of molecule 6, or with the monomer, molecule 7, to form a chain molecule or with the other end of the same molecule to form a ring, in this case using the diagonal from one vertex of a cube through the center of the other. Cyclization is thus in competition with step growth whenever the two ends of a chain polymer are found to be adjacent to each other. Rings were recognized as those molecules with equal numbers of bonds and residues. At the edges of the system of 20 × 20 × 20 units used in this study periodic boundary conditions applied.

Bonds do not dissociate, so the system evolves subject to kinetic considerations, but excluded volume constraints and simple configurational ideas prevail. Records of the links created at each lattice site allow us to analyze the system for the different types of molecules present, and to obtain the configurational properties of each molecule. The program has been written in two- and three-dimensional versions, in each case one vector being used to store the information for each element of the lattice, but two different short and simple functions are employed to map the neighbors for each representation.[29] The code of the two-dimensional representation has a dynamic graphical display of the lattice so that the model may be observed running, or at intervals one may inspect printed copies. This has allowed us to check the details of the procedures for model evolution and for the analysis. The two-dimensional version gave the same results as an earlier and differently-constructed program (that had been checked in the same manner during its development).[24] Full details of the Pascal program will be reported elsewhere.[30]

We have also performed enumeration studies on the oligomeric rings and chains, identifying all the possible distinct configurations on the 26-choice lattice: for example there are 26 possible orientations of the single bond of a dimer and 26 × 25 possible orientations of the two bonds of a linear trimer. The mean values of the configurational characteristics, $\langle R_c^2\rangle$ and $\langle S_c^2\rangle$ for the set of chains and of $\langle S_r^2\rangle$ for the rings were then obtained, R being the end-to-end distance of a chain and S being the residues of gyration.[2] The results of this study are entered in Table 1 and will be used when assessing the numerical and configurational statistics.

Table 1. Enumeration of Configurations of Small Chains and Rings on the 26-Choice Lattice

			Chains		
no. of bonds	1	2	3	4	5
no. of residues	2	3	4	5	6
no. of configurations	26	650	15 914	384 816	9 237 980
$\langle R_c^2\rangle$	2.077	4.320	6.702	9.206	11.735
$\langle S_c^2\rangle$	0.5192	0.9415	1.3559	1.7764	2.2178
$\langle R_c^2\rangle_{nc}$[a]		5.854	8.349	10.634	
$\langle S_c^2\rangle_{nc}$[a]		1.1710	1.5307	1.9183	
			Rings		
no. of bonds			3	4	5
no. of residues			3	4	5
no. of configurations			264	4178	64 256
$\langle S_r^2\rangle$			0.606 06	0.864 77	1.068 50
			Ratios[b]		
$C = \langle R_c^2\rangle/(n-1)\langle l^2\rangle$	1.000	1.040	1.0757	1.1081	1.1300
$D = \langle S_c^2\rangle/\langle R_c^2\rangle$	0.2500	0.2179	0.2023	0.1930	0.1891
$Z = \langle S_r^2\rangle/\langle S_c^2\rangle$			0.4470	0.4868	0.4814
$Y_R = \langle R_c^2\rangle_{nc}/\langle R_c^2\rangle$		1.355	1.246	1.155	
$Y_S = \langle S_c^2\rangle_{nc}/\langle S_c^2\rangle$		1.244	1.129	1.080	

[a] nc are noncyclizable chains or rings. [b] C, D, and Z are defined in eqs 8–10.[2,39,40] Y_R and Y_S are defined here.

Results and Discussion

(A) General Considerations. Trial simulations were performed with four different sizes of system, the sides of the cubes being 5, 10, 20, and 40 lengths, and the weight fractions of the ring components were obtained. For these systems the weight fractions at the end of the simulations were found to be respectively 0.23 (±0.03), 0.056 (±0.007),[25] 0.0395 (±0.0016), and 0.0387 (±0.0006). The measures of ring formation differ so much because not only were true rings counted but also the ambiguous species that joined ends after having passed through the periodic boundaries. They also, having equal numbers of bonds and residues, were counted as rings. The chance of this happening was high for the smallest system but was considered negligible for the two larger systems, for their behaviors, by this measure, were similar. Our study was therefore performed with the 20 × 20 × 20 system, using 25 repeats of runs of 50 simulations, to obtain statistical averages that are displayed in the figures.

Initially, oligomers form and grow regularly, and rings and long chains slowly emerge. The curve of p against time on a logarithmic scale is sigmoidal,[24,25] reflecting the manner in which the chemical change peters out as the remaining functional groups become isolated within a matrix of chain and ring segments. The extent of reaction, p, after 10 M and 20 M time units was not significantly different, nor was it much changed by causing all end groups to link to any unreacted neighbors. The limiting value was 0.983 33 (±0.000 02). For the molecules that have formed, the mean degree of polymerization, from eq 1, the Carothers function, is $1/(1-p) = 59.99$ (±0.07). These numbers are both higher than the values we obtained for the similar study on a two-dimensional eight-choice lattice[24] ($p = 0.945$ (±0.01) and $\langle n\rangle = 18.2$ (±0.4)); in the present 26-choice case the larger number of neighbors to a reactive site on the three-dimensional lattice apparently provides more opportunity for reaction, or less scope for screening other end groups by sites that have joined rings or become the midgroups of chains.

At the limit of the reaction the fraction of molecules that had formed rings was 0.291 (±0.007), a number only a little less than the value of 0.337 (±0.017) we obtained in our study of the problem on a similar two-dimensional lattice.[5] In three dimensions the limiting value of the weight of material that has entered rings by the time the process has ceased is 0.056 (±0.005),

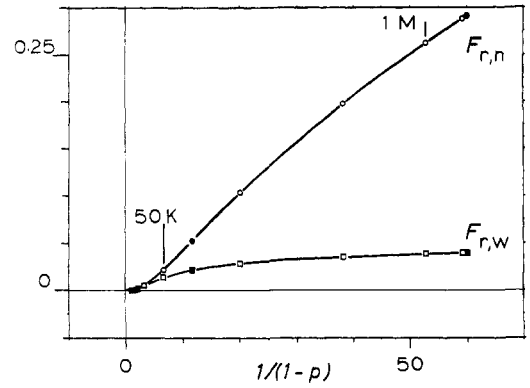

Figure 2. Plots of the number and weight fractions of rings, $F_{r,n}$ and $F_{r,w}$ respectively, against the Carothers function as the polymerization proceeds.

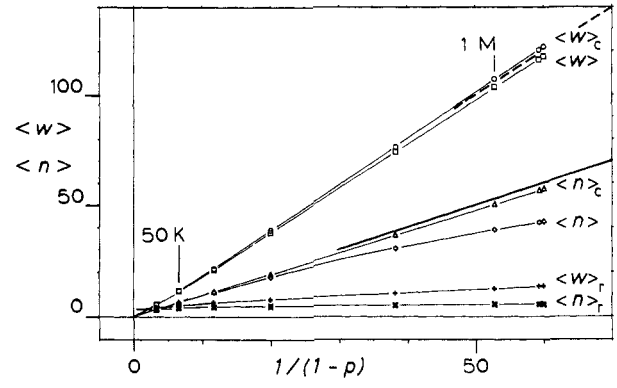

Figure 3. Plots against the Carothers function of the number average, $\langle n \rangle$, and the weight average, $\langle w \rangle$ size, of all the species and of the rings and chain components separately. The last two or three points coincide. The marks 50K and 1M indicate the times required for the simulation to reach the points. The heavy line shows the locus of points for which $\langle n \rangle = 1/(1-p)$, and the dashed line, that for which $\langle w \rangle = 2/(1-p)$.

which is a good deal less than the value of 0.141 (±0.007) found in two dimensions.[24] From the disparities of the weight and number fractions of rings it appears that the mean size of the chains is much greater than that of the rings in the three-dimensional study.

We show the values of the number and weight fractions of rings, $F_{r,n}$ and $F_{r,w}$ respectively plotted in Figure 2 against the Carothers function, $1/(1-p)$, which we use for convenience to display the developments. The more conventional parameter, the extent of reaction, p, was obtained from N_b/N_0,[24] the ratio of the number of bonds formed to the number of monomers initially present. The numbers placed against the $F_{r,w}$ curve are the corresponding time values. The points on the curves are closely spaced when reaction times are short because, from the form of the function, $1/(1-p)$ rises only slowly while p changes through the first part of its range, and at the end of the process the spacings again diminish when the scope for further reactions peters out. Ring formation does not occur to a significant extent until the extent of reaction is above 0.5, since only then does a reasonable proportion of oligomers exist from which rings might form. The form of these two plots shows that both $F_{r,n}$ and $F_{r,w}$ are rising progressively with the progress of the reaction. The rise ceases only because the process is terminated by the isolation of functional groups. The former function rises faster than that latter as the mean size of the two types of species differ, as we now discuss.

The number average mean size of the molecules, and of the rings and chains separately, are shown as a function of the Carothers function in Figure 3, together with the corresponding weight averages for the substances. We have noted[24] that there is a simple relationship between the number of bonds that form, N_b, the number of rings, N_r, the number of residues N_0, and the number of molecules, N_t, at time t:[24]

$$N_0 + N_r = N_b + N_t \tag{3}$$

This equation expresses the fact that when one ring forms the number of bonds rises by 1, and $p = N_b/N_0$ rises but the mean size of the molecules, $\langle n \rangle = N_0/N_t$, is not altered. The points for $\langle n \rangle$ initially follow the diagonal, which we have marked with a heavy line, but deviations then occur as rings form. On our plot, the curve for the chain component terminates at 57.6 (±0.7). It falls below the diagonal, for the value of p in the Carothers function corresponds to the value for the system rather than just the chains. The curve for the rings starts, as it must, at 3, for only such rings form initially, and for a while it exceeds that of the chains, but it rises less rapidly as the reaction proceeds and it terminates at 5.77 (±0.17). The fact that all the $\langle n \rangle$ curves lie below the diagonal and that there is a curve for rings reflects ring formation. The curves for the weight averages all lie well above the corresponding number averages, for the distributions are polydisperse, $z = \langle w \rangle / \langle n \rangle$ finally being 2.33 (±0.36) for the rings and 2.12 (±0.04) for the chains, in consequence of which $\langle w \rangle_c$ lies slightly above the ideal line of $\langle w \rangle = 2/(1-p)$. z is even larger for the rings and chains combined, being 2.77 (±0.06), as the values of $\langle n \rangle$ and $\langle w \rangle$ are respectively 42.5 (±0.6) and 117.7 (±2.4) at the end of the simulation.

(B) Distribution Functions of the Ring, Chain, and Total Populations. The number and weight distributions of all the species present and of the chains and rings separately are shown in Figures 4–7 for two selected times during the reaction and for the final state achieved. (The corresponding points are shown solid on Figure 2.) The distribution functions are scattered at the end of the reaction and for large species which are fewer in number because of the Monte-Carlo origin of the data. On Figure 4–c close to the data for the chains lie dashed lines obtained with eq 2, using the value of p provided by N_b/N_0. There is a steady decrease in chain number as n rises at all values of p, except for a few points at the start of the latter plot. For the final set of data in Figure 4c we obtained the full line with $p_c = (\langle n \rangle_c - 1)/\langle n \rangle_c$ and $N_{c,0}$ (the number of residues in the chain fraction) instead of p and N_0, respectively. This employment of eq 4 appears to give a better fit than eq 2.

$$N_{c,n} = N_{c,0}(1-p_c)^2 p_c^{n-1} \tag{4}$$

To appraise the fit further we introduce and plot residuals, X_n, the Monte-Carlo results less an approriate theoretical expression. The residuals are shown in the lower part of Figure 4: to begin with, as in (d), monomers are depleted and the next oligomers are in excess, and then the excess settles down. At the end of the reaction the monomers are in relative excess and the next oligomers are depleted. The data of part e show a good fit once $n > 10$ because we have used eq 4. The perturbations are apparently relatively small and seem to be concentrated at the start of the distributions. In fact the number distribution is rather insensitive to any distortion of the distribution function except at low

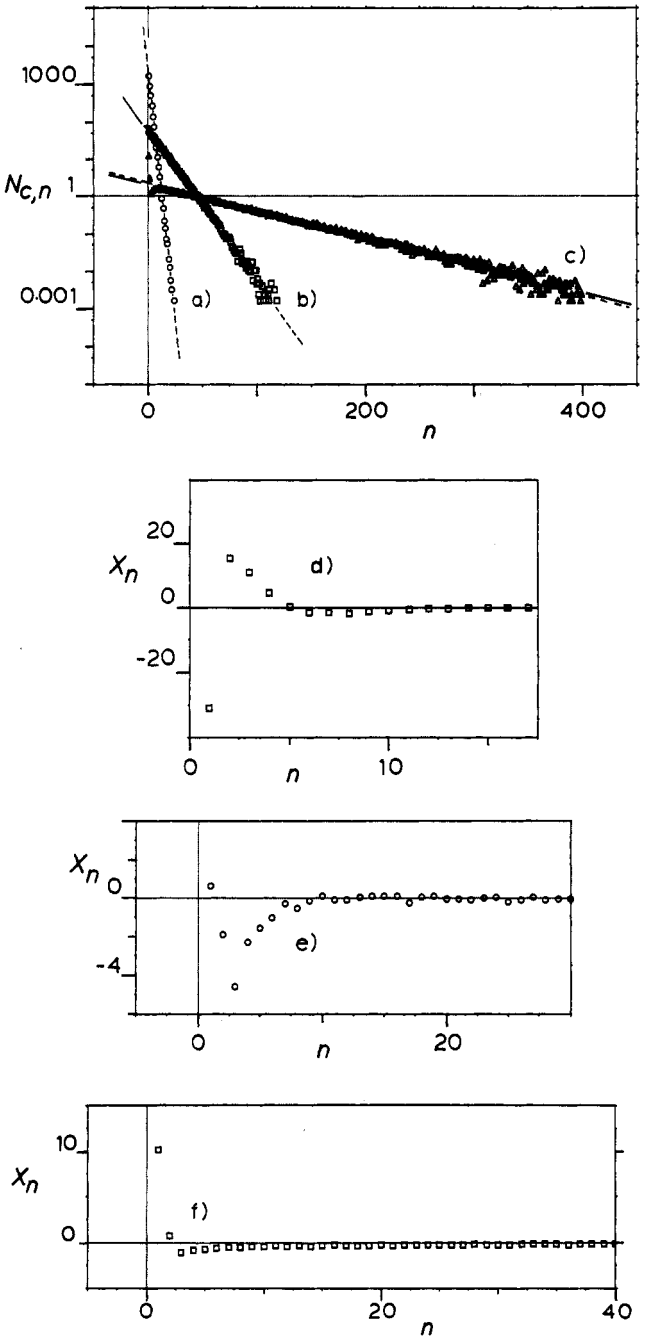

Figure 4. Number distributions for the chains present at three stages of the simulation: (a) $t = 10\,000$, $p = 0.545\,15$; (b) $t = 100\,000$, $p = 0.914\,75$; (c) completion, $p = 0.983\,33$. The dashed lines are eq 2. The full line uses instead the value of p_c obtained from the chain component. Residuals, X_n, the Monte-Carlo values—the function values, are plotted in (d) time = 10 000, $p = 0.545\,15$ (eq 2), (e) time = 100 000, $p_c = 0.912\,89$ (eq 4), and (f) completion, $p_c = 0.982\,64$ (eq 4).

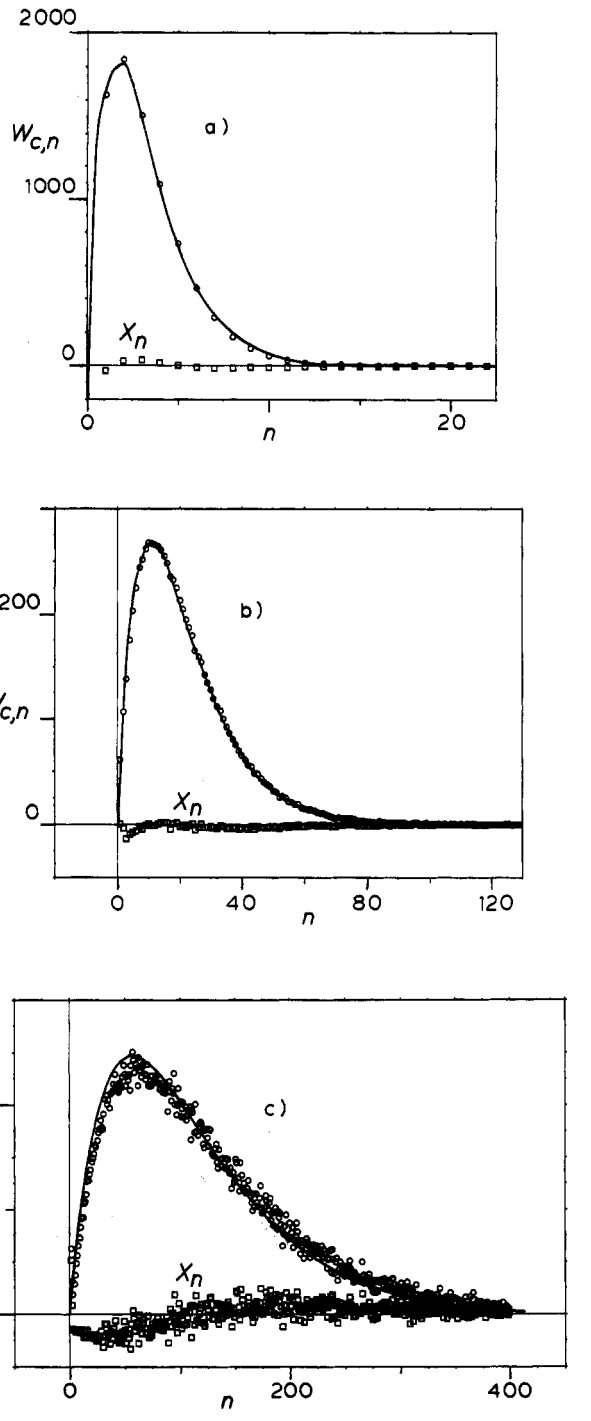

Figure 5. Weight distribution functions for the chains present at three stages of the simulation: (a) $t = 10\,000$, $p = 0.545\,15$, $p_c = 0.544\,29$; (b) $t = 100\,000$, $p = 0.9148$, $p_c = 0.912\,89$; (c) completion, $p = 0.983\,33$, $p_c = 0.982\,64$. The curves are eq 4 with the indicated values of p_c and the appropriate value of $N_{c,0}$. Residuals, X_n, the Monte-Carlo values—the p-function values (eq 5), are plotted below each curve.

values of n; the weight distribution functions are more sensitive to the distortions that are found at higher n values.

Weight distribution curves are shown for the chain component in Figure 5. The solid curves shown there for the weight distributions were obtained using a modification of the standard form[2,3] that we have adapted to be appropriate to the chain fraction by itself:

$$W_{c,n} = N_{c,0}(1 - p_c)^2 n p_c^{n-1} \qquad (5)$$

The fit in parts a and b are good, so the model reproduces fairly faithfully the chief features of chain formation in three dimensions at low extents of reaction, though the perturbations noted when discussing the number distribution are still present. In the plot for the end of the reaction of Figure 5c for low values of n the experimental values are not well fitted by the curve: monomers and dimers are in excess, there is a depletion at low values and an excess at high values. The areas above and below the abscissa of the residue plot are equal. The excess of monomers and dimers is relatively pronounced, and we consider this to be a

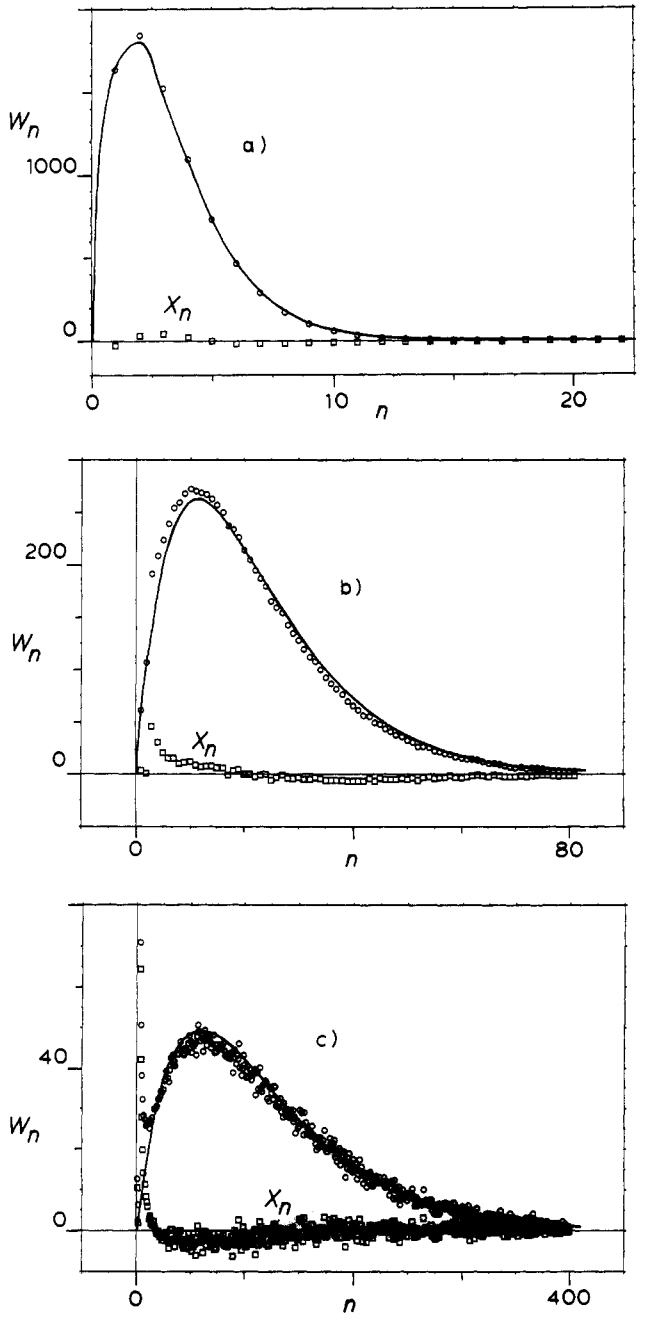

Figure 6. Weight distributions for the species present at three stages of the simulation: (a) $t = 10\,000$, $p = 0.545\,15$; (b) $t = 100\,000$, $p = 0.9148$; (c) completion, $p = 0.983\,33$. The dashed curves are eq 2 with the preceding values of p. Residuals, X_n, the Monte-Carlo values—the p-function values (eq 6), are plotted below each curve and show systematic variations.

consequence of the manner in which the next oligomers have become depleted by ring formation rather than reflecting just their isolation and inability to grow further—after all the monomers and dimer ends are likely to be less screened from other end groups by the remainder of the molecules than are the end groups of longer molecules. The size of this effect is not surprising, for the entries of Table 1 show that a proportion of about 0.41 of the trimer chains might cyclize at any instance, there being 264 out of the possible 650 configurations that have end groups on adjacent sites. Similarly, about 0.26 (4178/15914) of the tetramer chains and 0.17 (64256/384816) of the pentamer chains have configurations that might cyclize. This proportion decreases as the chain size rises but represents a continuous elimination of the low molecular weight

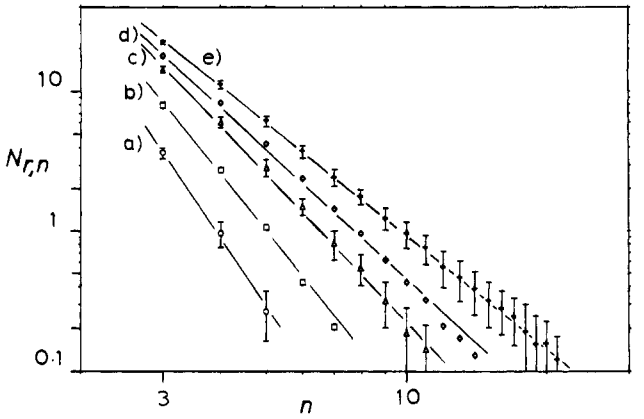

Figure 7. Number distributions for the ring species present at the stages of the simulation indicated: (a) $t = 10\,000$, $p = 0.545\,15$; (b) $t = 20\,000$, $p = 0.700\,87$; (c) $t = 50\,000$, $p = 0.849\,17$; (d) $t = 100\,000$, $p = 0.91\,48$; (e) completion, $p = 0.983\,33$. The errors are one standard deviation. The lines are in the form of eq 5.

materials throughout the reaction period. The effect seems to extend up to $n \sim 100$. There is an excess of molecules with $n > 120$. The consequences, as we have noted, are that the polydispersity is higher (2.12) than the ideal value of 2.00.

In Figure 6 we show the weight distributions for all the species, characterized by size n irrespective of them being rings or chains. We show the solid curve obtained from the usual function,[2,3] eq 6

$$W_{c,n} = N_0(1-p)^2 np^{n-1} \tag{6}$$

The plot at low conversion, Figure 6a, shows good agreement between results and the standard expression, but in Figure 6b there are clearly systematic errors associated with ring production that lead to a sharpening of the Monte-Carlo distribution. Conversely, on the plot of Figure 6c we may see that the ring formation feature, being much more intense, is now resolved at low values of n, for the main ring components now give a broad peak at much higher values of n. The formation of chains has led to a depletion of the rings near the broad maximum and there is a slight excess on the side of the peak above that. The consequence is, as we have noted, a significantly high value (2.77) for the polydispersity.

We display the ring number distribution functions, $N_{r,n}$ at five stages of the reactions in Figure 7, logarithmic scales being adopted as suggested by the form of the equilibrium distribution function.[4] They show, especially at the start of the process, how the number of ring molecules diminishes sharply with ring size, and within the tolerance of the standard deviations the data fall very close to straight lines. We have fitted eq 7 to each set of the data at seven stages of the polymerization using the NAG routine EO4 FCF,[31]

$$N_{r,n} = A_0 n^{-\gamma} \tag{7}$$

weighting the square of each residual according to the square of the reciprocal of the standard deviation of data.[32] At the limiting state (as indistinguishably at time = 20 000 000) the slope had a value of -2.65 (± 0.03). Apart from the point for the three-membered rings, which lies a little below the trend, a straight line provides a good representation of the results. If we omit the first point, the value of γ is only slightly higher,

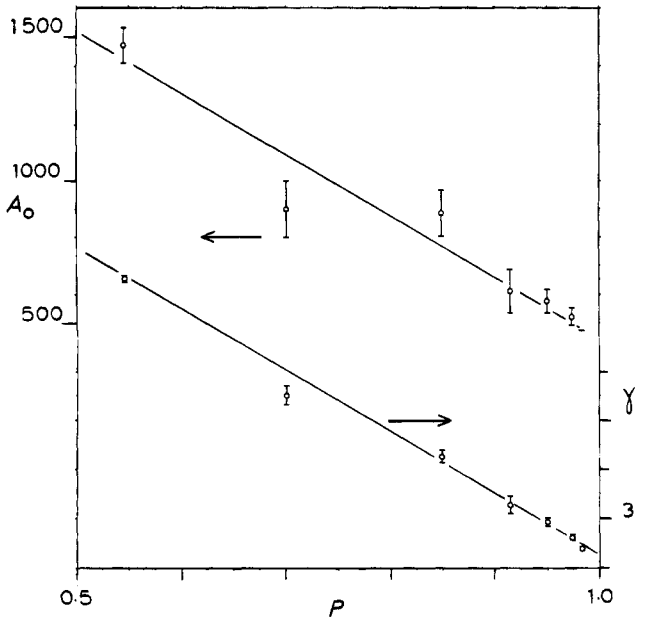

Figure 8. Plots of the γ and A_0 parameters of eq 7 for the ring distributions against the extent of reaction, p.

−2.68 (±0.02). We plot the exponents of each ring distribution function against p for the second part of the polymerization in Figure 8, where it may be seen that the points lie close to a straight line (as was found in the two-dimension study[25]). The equation that describes this line is $\gamma = 8.875 - 6.250p$. The A_0 parameter over the same range is similarly given by $A_0 = 2590 - 2040p$.

The limiting values of γ are both higher than the value appropriate to an equilibrium distribution,[4] −2.50. Curiously, the present values are also very close to that obtained in the study on the eight-choice two-dimensional lattice, −2.73 (±0.02),[24] which compared less well with the appropriate equilibrium value of −2.00. Thus our three-dimensional limiting value of γ is closer to the equilibrium value than was the two-dimensional value. This effect survives if we extrapolate to $p = 1.00$, the limiting values in two and three dimensions then being −2.40[24] and −2.625. The discrepancy between the limiting values of the kinetic studies and the equilibrium values appears to be associated with the dimensionality of the problem rather than the details of the lattice representation.

(C) Configurations of Ring and Chain Species. The growth process adopted in the present lattice-bound study differs from that of the classical nonreturning random walk problem,[21,33-35] in that growth takes place at one end of the chain, but to retain proper sampling statistics, a random growth that would lead to a double occupancy of a site causes the configuration to be rejected. This attrition accumulates and is severe for long chains,[33] yet such chains are needed to establish limiting tendencies for the behavior of the isolated chain in an athermal solvent. Attrition was ameliorated by Wall and Erpenbeck with their chain enrichment process[35] that *inter alia* led to the recognition of the result $\langle R_c^2 \rangle \sim (n-1)^{\nu}$, with ν slightly less than 1.20[21] (R_c being the end-to-end distance). Such lattice Monte-Carlo studies stimulated the application of renormalization group theory[21] to the problem, and led to the confirmation of this result for the isolated chain. The related issue of the configurational statistics of linear polymers in the bulk, noncrystalline state was suggested in Flory's work to be equivalent to Θ solution conditions, and to have the form $\langle R_c^2 \rangle \sim (n-1)$,[1,00] the presence of adjacent chains leading to a shielding or suppression of the long range intramolecular excluded volume effect. Experimental results[36,37] are consistent with this idea. Mansfield's lattice simulation,[38] that used an ingenious, metathesis, approach when all lattice sites were occupied to vary the structures and so to produce new long chains with new random configurations, has confirmed Flory's theorem that the exponent is unity,[2] the M-C results providing a slightly higher value (1.03 ± 0.01), perhaps because the molecular weights were not very large. In neither of these approaches[21,33-35,38] did the configurations of the polymers change to sample configurational space.

In the present simulation the chains form gradually from single units as true random self-avoiding walks, but they are short to begin with. As time lapses the first molecules grow by reactions with other oligomers and new oligomers develop in the interstices: the growth process of the latter molecules and thus their configurations must be influenced by the presence of the previously-formed chains, the effect operating through limiting scope for reactions at an end group. The consequences are not immediately obvious and are to be established. The depletion of compact chains by ring formation may also raise mean chain configurations. The configurations are frozen by the kinetic process, both as the structures form while the reaction proceeds and finally as the scope for further growth fails. The structures are fixed in position, for no movements are employed, as in the other models,[21,33-35,38] but this does not prevent the evolution of configurational characteristics of molecules of any particular size or type as the reaction proceeds: the mean dimensions of a linear decamer, for example, may well be altered as the reaction proceeds, for old ones react and new ones form. In what may be regarded as the production of semidilute conditions, any mean field effect that operates on the configurations does this merely through the choice of which end groups are to combine to create larger molecules. A full understanding of the growth process requires an understanding of the chain configurations.

To assist in an understanding of the effects of ring formation, we have enumerated all the chains and rings that have up to 6 residues and have obtained mean values of the configurational characteristics, and entered these in Table 1. These values are close to the Monte-Carlo results at the start of the reaction. For example, when $p = 0.110$, the values of $\langle R^2 \rangle$ and $\langle S^2 \rangle$ of the trimers, tetramers, and pentamers are within 1% of the enumerated values. For ring molecules with 3, 4, or 5 residues the configurations correspond to a subset of chains: thus of the 650 configurations of the chain molecule with 3 residues, 264 might be made into a ring by the formation of one more bond. If this were to happen, the mean value $\langle Sc^2 \rangle$ would rise to 1.1710, that is by a factor, Y_s, of 1.244. This is the ratio of the mean configuration of the chains that cannot cyclize to that of the chains, $\langle S_c^2 \rangle_{nc}/\langle S_c^2 \rangle$.

For the analysis of the Monte-Carlo data we take as an initial reference the relationship for the random flight of $n-1$ bonds[2] (n being the number of residues)

$$\langle R_c^2 \rangle = (n-1)\langle l^2 \rangle \tag{8}$$

Two other results may also be used as a guide, that of Debye for chains in a random flight concerning their

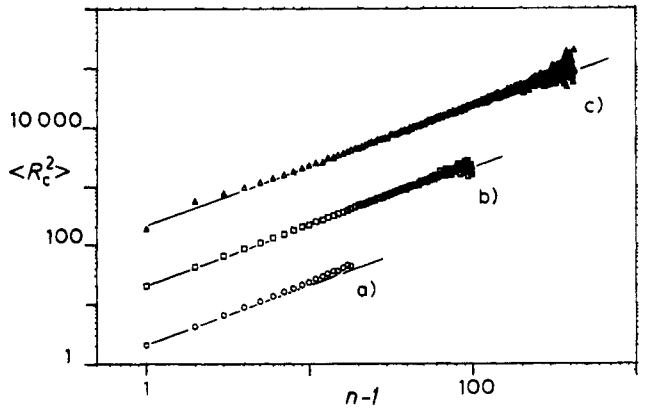

Figure 9. Plots of $\langle R_c^2 \rangle$ against the number of bonds for the chains at (a) $t = 10\,000$, $p = 0.545\,15$; (b) $t = 100\,000$, $p = 0.9148$; (c) completion, $p = 0.983\,33$. The lines correspond to the freely jointed chain of eq 8. The upper plots have been displaced by one or two decades.

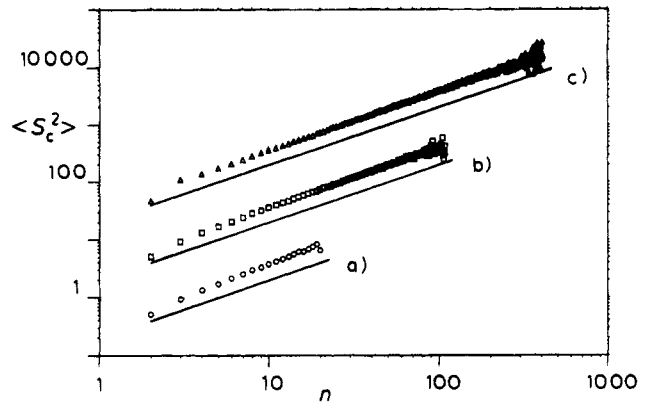

Figure 10. Plots of $\langle S_c^2 \rangle$ against the number of residues for the chains at (a) $t = 10\,000$, $p = 0.545\,15$; (b) $t = 100\,000$, $p = 0.9148$; (c) completion, $p = 0.983\,33$. The lines correspond to the freely jointed chain of eq 8 and 9. The upper plots have been displaced by one or two decades.

mean square radius of gyration,[39] $\langle S_c^2 \rangle$:

$$\langle S_c^2 \rangle / \langle R_c^2 \rangle = {}^1/_6 \tag{9}$$

and that of Zimm and Stockmayer[40] (supported by experiment[14]) which links the radius of gyration of a ring to that of a chain of the same number of bonds:

$$\langle S_r^2 \rangle / \langle S_c^2 \rangle = {}^1/_2 \tag{10}$$

We enter in the table the values for the oligomers of the characteristic ratio $C = \langle R_c^2 \rangle / n \langle l^2 \rangle$, the Debye ratio $D = \langle S_c^2 \rangle / \langle R_c^2 \rangle$, and the Stockmayer–Zimm ratio $Z = \langle S_c^2 \rangle / \langle S_c^2 \rangle$ and note that they are not ideal, presumably because the number of lattice configurations is rather small.

We plot in Figures 9–11 values of $\langle R_c^2 \rangle$ and $\langle S_c^2 \rangle$ (for the chains) and of $\langle S_r^2 \rangle$ (for the rings) at three sample stages of the polymerization process, when the p values were about 0.55, 0.91, and 0.98 (at infinite time). The flare or scatter at the end of each curve reflects the imprecision in these points caused by the low populations of such species and the larger possible range of sizes. (We have not plotted data beyond this point.) The sizes of the oligomers are highly precise, but the sizes of the larger species are less so, particularly for the rings, for there are fewer of them and their range of sizes may be greater. For example at the end of the

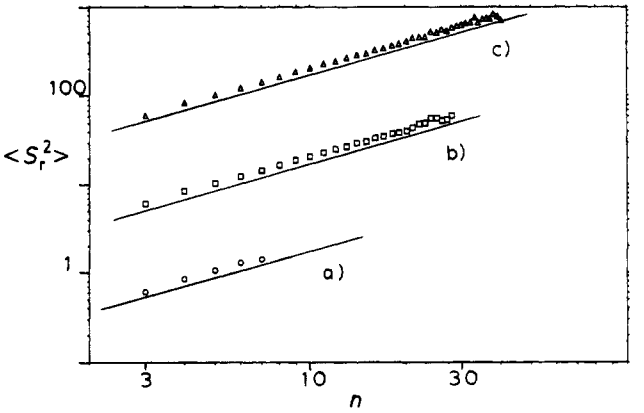

Figure 11. Plots of $\langle S_r^2 \rangle$ against the number of residues for the rings at (a) $t = 10\,000$, $p = 0.545\,15$; (b) $t = 100\,000$, $p = 0.9148$; (c) completion, $p = 0.983\,33$. The lines correspond to the freely jointed chain of eqs 8–10. The upper plots have been displaced by one or two decades.

simulation $\langle R_c^2 \rangle$, $\langle S_c^2 \rangle$, and $\langle S_r^2 \rangle$ were found to be respectively 1.895 (±0.012), 1.112 (±0.009), and 0.6010 (±0.0002) for molecules with 3 residues, and 65.8 (±1.5), 11.18 (±1.15), and 6.32 (±1.32) for molecules with 30 residues. The perturbations caused by ring formation and the structure of the errors mean that when we attempt to obtain the slopes of our plots, the values are sensitive to the choice we make of the first points to include within the fit.

As a guide to analysis we have placed upon each plot of $\langle R_c^2 \rangle$ in Figure 9 the line expected from eq 8, for the freely jointed chain. In general the points lie close above the lines, there being one clear exception, that for the single bond of the dimer at the end of the process. Its value has been reduced slightly from values close to $\langle l^2 \rangle = 54/26 = 2.077$ (as in Table 1, for the dimer) to 1.895 (±0.012), presumably because the more extended configurations of the dimer react more frequently, and because bonds on diagonals form less frequently on account of the local excluded volume effect caused by adjacent molecules late in the reaction. The perturbations to curve c at $n = 2$ to about 7, characterized by significant excesses in $\langle R_c^2 \rangle$ are attributed to the effect of ring formation: compact and cyclizable chains have been depleted from the sample and have not been replenished by subsequent growth. We have quantified this by the parameter Y_R for the enumeration studies summarized in Table 1, which measures the proportional increase in $\langle R_c^2 \rangle$ for a particular oligomeric chain when the chain configurations that might lead to a ring by one further chemical reaction are removed. We see that Y_R decreases from 1.355 when $n = 3$ to 1.155 when $n = 5$, and presumably falls further toward unity as n rises. From a comparison of the dimensions of the chains when $p = 0.110$ and at the end of the reaction the Monte-Carlo results give ratios of 1.308, 1.126, and 1.062 for trimer, tetramer, and pentamer, respectively. Thus the simulation shows a greater fall in this factor than the enumeration.

Values of $\langle R_c^2 \rangle$ are close to the ideal line at the start of the reaction, but they drift above the line as n rises. The slope on the lower curve of Figure 9 ($p = 0.545$) is about 1.11 if the first four points are neglected to allow for possible effects from ring formation; for the second curve, when the first five points are omitted, the slope is about 1.05. The data for the limiting case of $p = 0.983\,33$, once we move away from the first 10 points that may be affected by the ring formation perturbation,

shows a smaller slope of about 1.03. Never is γ as large as 1.20 in the data we have examined. Thus as the medium in which the chains are placed becomes richer in oligomers and then in other chains and rings there is a tendency for the slope to decrease toward the bulk phase value of unity.[2,38] Our process is growing chains has produced configurational exponents similar to that of Mansfield.[38]

The values of $\langle S_c^2 \rangle$ (for the chains) are displayed in Figure 10 at the same three stages of the reaction: they lie above the straight lines obtained using eqs 8 and 9. As the reaction proceeds, the point for the dimer falls relatively as long diagonal molecules fail to form, and the point for trimers rises relatively from the depletion of cyclizable chains. Again we refer to Table 1, where Y_s values of the enumerations indicate that the effect diminishes from 1.244 to 1.080 as we move from 3 to 5 bond chains. The comparable values obtained in the simulation, by dividing $\langle S_c^2 \rangle$ values at the end with those near the start of the simulation are 1.1845, 1.0528, and 1.0138: the simulation is less affected than the enumeration, and the resulting perturbation falls more quickly. It masks to some extent the smooth rise shown in curve c. If $n > 8$ the points of that curve lie well on a line which has a slope just above 1.00 (1.04 ± 0.02). For the chains when $p = 0.55$, the exponent is 1.17 (±0.01) if the first two points are omitted, nearly as much as the value, 1.2, that has been attributed to chains subject to excluded volume conditions.[23,38] At the intermediate stage the data of curve b tend toward the ideal slope from below: for points with $N > 5$, $\gamma = 1.08$ (±0.02).

The configurational characteristic of the rings, $\langle S_r^2 \rangle$, are displayed in Figure 11 for the three stages of the reaction. Each set of points lies a little above the ideal line produced by combining eqs 8–10, and each set seems to lie on a straight line. Even the point for the three-membered rings is on the general trend. The fits we obtained for Figure 11a are sensitive to the number of points chosen. If we omit the cyclic trimers and tetramers, analysis shows that the slope for the upper two curves is 1.02 (±0.02), close to the value for the ideal ring.

In order to further the analysis the Debye ratio $D = \langle S_c^2 \rangle / \langle R_c^2 \rangle$ and the Zimm–Stockmayer ratio $Z \langle S_r^2 \rangle / \langle S_c^2 \rangle$ are plotted for the final products of the reactions in Figure 12a,b. The former falls toward the value of $^1/_6$, and the average for the last 75 points of the plot is 0.168 (±0.05). This is clearly greater than the value of 0.157 found for self-avoiding walks.[35] The result does not mean that the chains are Gaussian in their configurations: a similar ratio has been obtained for chains on a lattice subject to the self-avoiding walk condition and whose configurations have been compacted to the Θ condition by weighting long range contacts.[41] In this study the presence of the matrix molecules has apparently a similar effect upon this measure of configurational properties.

In contrast the Zimm ratio at the end of the polymerization has a limiting value that is not ideal. From an initial low value the curve for $\langle S_r^2 \rangle / \langle S_c^2 \rangle$ passes through the ideal value of 0.50, and apparently when the number of bonds is greater than 10 and the points become rather scattered, the mean ratio settles to about 0.52–0.54: for the last 20 points the mean value is 0.53 (±0.02). Perhaps this reflects a greater sensitivity of $\langle S_r^2 \rangle$ values to the residual excluded volume effect than

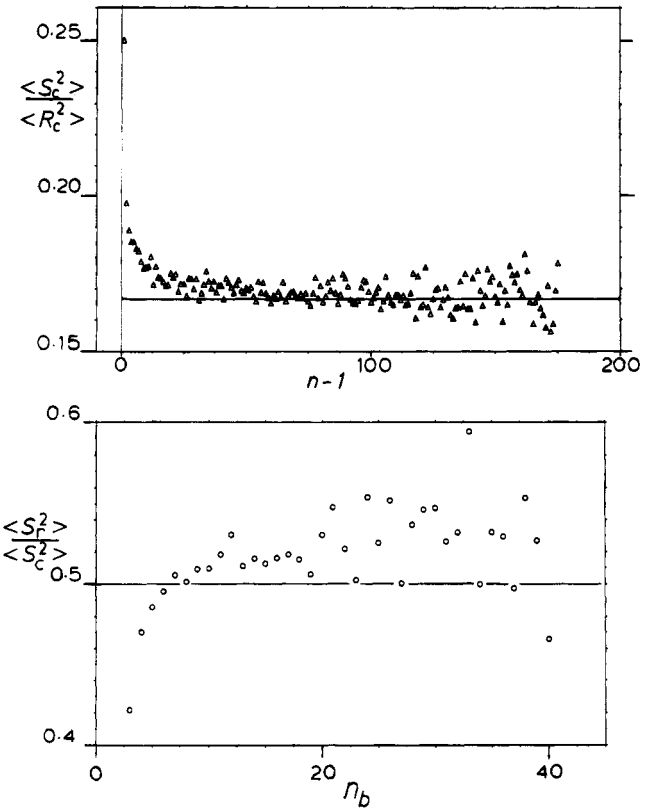

Figure 12. Plots of (a) the Debye ratio, $\langle S_c^2 \rangle / \langle R_c^2 \rangle$ against the molecular size and (b) the Zimm–Stockmayer ratio $\langle S_r^2 \rangle / \langle S_c^2 \rangle$ against the number of bonds in the molecule, for the final products of the reactions.

of the $\langle S_c^2 \rangle$, a point noted in some experimental studies.[14]

Conclusions

Our simulations permit the competition between chain growth and ring formation to be modeled on a lattice using a step growth model of irreversible bond formation. The manner in which chains grow is characterized by number distributions that are very close to the standard Flory function by eq 2 when the extent of the reaction is low, and the weight distribution functions within the class of chains that form (eq 5) are also closely followed, though minor discrepancies do occur. These and the major discrepancies that emerge toward the end of the process are attributable to the formation and development of a ring population, to the extent that 29% of the molecules are rings. (A real system[19,20] might have more, since our model neglects rings from monomers and dimers). Despite the rings being a much smaller fraction of the mass of the system (4%) they are in a proportion which is so extensive that the weight distribution for all the species, W_n, in the system becomes bimodal, and the polydispersity, z, rises to 2.8. The ring number distribution functions have been shown to follow a negative power law, the diminution in ring number with n becoming less severe as rings accumulate from the larger chains that eventually form. The final exponent, −2.65, is closer to the equilibrium value of −2.50 than was the case in two dimensions.

The configurations of the species that are present at a particular time are fixed by the step growth reactions that created each bond within each particular molecule. The configurations are quite close to the behavior of the ideal random chain, but significant deviations have been found. For the oligomeric chains, particularly toward

the end of the reaction, there is a major perturbation in $\langle R_c^2 \rangle$ and in $\langle S_c^2 \rangle$ caused by the formation of three-membered and larger rings, a process that depletes the more compact configurations of the chains but becomes less important for larger molecules, as enumeration and inspection have shown. Away from the region affected by this the configurations expand with the size according to the familiar scaling laws, the exponents of n becoming closer to 1.00 than to 1.20 as the reaction approaches completion. The manner in which the (frozen) configurations are created in this step growth model, by a random choice of sites to be linked by a bond, results in molecules whose configurations approach in behavior that of the Flory Θ condition when the extent of reaction is high.

Acknowledgment. We thank The Queen's University of Belfast for an HP710 microcomputer. R.A.W.M. thanks QUBIS for support during part of the period of the work and David Gault for assistance.

References and Notes

(1) *Collected Papers of W. H. Carothers on High Polymeric Substances;* Mark, H., Whitby, G. S., Eds.; Vol. 1 of High Polymers; Interscience: New York, 1940.
(2) Flory, P. J. *Principles of Polymer Chemistry*; Cornell: Ithaca, NY, 1953.
(3) Flory, P. J. *J. Am. Chem. Soc.* **1936**, *58*, 1877.
(4) Jacobsen, H.; Stockmayer, W. H. *J. Chem. Phys.* **1950**, *18*, 1600.
(5) Flory, P. J. *Statistical Mechanics of Chain Molecules*; Interscience: New York, 1969.
(6) Griffiths, A. J. F.; Miller, J. H.; Suzuki, D. T.; Lewontin, R. C., Gelbart, W. M. *An Introduction to Genetic Analysis*, 5th ed.; Freeman & Co.: New York, 1993; p 415.
(7) Hild, G.; Strazielle, C.; Rempp, P. *Eur. Polym. J.* **1983**, *19*, 721.
(8) Roovers, J. E.; Toporowski, P. M. *Macromolecules* **1983**, *16*, 842.
(9) Clarson, S. J.; Semlyn, J. A.; Dodgson, K. *Polymer* **1991**, *32*, 2823.
(10) Hogen-Esh, T. E.; Toreki, W. *Polym. Prepr. (Am. Chem. Soc., Div. Polym. Chem.)* **1988**, *30* (1), 129.
(11) Yang, A. J-M.; Di Marzio, E. A. *Macromolecules* **1991**, *24*, 6012.
(12) McKenna, G. B.; Hadziioannou, G.; Lutz, P.; Hild, C.; Strazielle, C.; Straupe, C.; Rempp, P.; Kovacs, A. J. *Macromolecules* **1987**, *20*, 513.
(13) Roovers, J. E. *Macromolecules* **1985**, *18*, 1359.
(14) Roovers, J. E. *J. Polym. Sci., Polym. Phys. Eds.* **1985**, *23*, 1117.
(15) Hodge, P.; Houghton, M. P.; Lee, M. S. K. *J. Chem. Soc., Chem. Commun.* **1993**, 581.
(16) Wood, B. R.; Semlyn, J. A.; Hodge, P. *Polymer* **1994**, *35*, 1542.
(17) Semlyn, J. A. *Pure Appl. Chem.* **1981**, *53*, 1797.
(18) *Cyclic Polymers*; Semlyn, J. A., Ed.; Elsevier: London, 1986.
(19) Morawetz, H.; Goodman, N. *Macromolecules* **1970**, *3*, 699.
(20) Ercolani, G.; Mandolini, L.; Mencarelli, P. *Macromolecules* **1988**, *21*, 1241.
(21) De Gennes, P. G. *Scaling Concepts in Polymer Physics*; Cornell: Ithaca, NY, 1979.
(22) Winnick, M. A. *Acc. Chem. Res.* **1985**, *18*, 73.
(23) ten Brinke, G.; Hadziioannou, G. *Macromolecules* **1987**, *20*, 480.
(24) Fawcett, A. H.; McBride, F. V.; Rutherford, J. *Macromolecules* **1989**, *22*, 4536.
(25) Fawcett, A. H.; McBride, F. V.; Mee, R. A. W. *Macromol. Chem. Theory Simul.* **1993**, *2*, 91.
(26) The plots of log $N_{c,n}$ against log n of our two-dimensional study[24] on an eight-choice lattice showed little evidence of oscillations about the trend that might be caused by lattice effects.
(27) Carmesin, I.; Kremer, K. *Macromolecules* **1988**, *21*, 2819.
(28) Iwata, K. *Macromolecules* **1985**, *18*, 116.
(29) The PASCAL computer language we have used allows one to define these neighbors as members of a single set, with 26 members in the three-dimensional version. We used the Pascal Plus random number generator and ran the programms on an HP710.
(30) McBride, F. V.; Mee, R. A. W.; Fawcett, A. H. Manuscript in preparation.
(31) NAG Routine EO4 FCF, Mark XV, revised 1991.
(32) Wolberg, J. R. *Prediction Analysis*; Van Nostrand: London, 1967.
(33) Hammersley, T. M.; Morton, K. W. *J. R. Stat. Soc. B* **1954**, *16*, 23.
(34) Bruns, W. In *Monte Carlo Applications to Polymer Science*; Bruns, W., Motoc, I., O'Driscoll, K. F., Eds.; Lecture Notes in Chemistry, 27; Springer-Verlag: Berlin, 1981, p 105.
(35) Wall, F. T.; Erpenbeck, J. J. *J. Chem. Phys.* **1959**, *30*, 634.
(36) Cotton, J. P.; Decker, H.; Benoit, B.; Farnoux, B.; Higgins, J.; Jannink, G.; Ober, R.; Picot, C.; des Cloiseaux, J. *Macromolecules* **1974**, *7*, 863.
(37) Kirste, R. G.; Kruse, W. A.; Ibel, K. *Polymer* **1975**, *16*, 120.
(38) Mansfield, M. L. *J. Chem. Phys.* **1982**, *77*, 1554.
(39) Debye, J. C. P. *J. Chem. Phys.* **1946**, *14*, 636.
(40) Zimm, B. H.; Stockmayer, W. *J. Chem. Phys.* **1949**, *17*, 1301.
(41) Bruns, W.; Carl, W. *Macromolecules* **1991**, *29*, 209.

MA9411282